IMPACT OF TP53 MUTATION ON TUMOR MICROENVIRONMENT IN HPV- HNSCC

by

Yuqi Kang

A thesis submitted to Johns Hopkins University in conformity with the requirements for the degree of Master of Science in Engineering

Baltimore, Maryland

May, 2021

Abstract

TP53 mutations are one of the most frequent genomic alterations in head and neck squamous cell carcinoma (HNSCC). Particularly, *TP53* mutations are observed in HPV negative (HPV-) HNSCC patients and have a strong association with poor prognosis. However, the effects of *TP53* mutations in tumor microenvironment (TME) have not been characterized in HNSCC. I assessed the extent of immune cell infiltrates among HPV- patients from the TCGA-HNSC Pan-Cancer Atlas dataset.

Patients were stratified based on their *TP53* mutation status and were evaluated for their TME and survival status. Gene differential expression and co-mutation comparative analysis were used to identify other co-factors to further elucidate phenotypic variability among HNSCC patients with different *TP53* mutation status. Gene set enrichment analysis were applied to identify relevant altered pathways.

HPV- HNSCC was found to be associated with poorer survival status and unfavorable TME, and more frequent *TP53* alterations. Among HPV- HNSCC patients, the unfavorable clinical outcome co-occurred with higher level of

M0 macrophage infiltration and lower level of T follicular helper cell infiltration. Patients with homozygous *TP53* mutation were shown to exhibit poorer survival status, which is shown to be exaggerated with the co-occurrence of *PIK3CA* mutations. I was able to identify immune-related pathways that were down-regulated and highlight gene interactions that might bring about the emergence of this immunosuppressive TME.

In conclusion, the poor prognosis associated with *TP53* mutation in HNSCC patients, was, at least partially, caused by the tumor driven suppression of immune response by the enrichment of macrophages and the deficiency of T cells. I identified a subset of HPV- HNSCC patients that associated with a higher risk of poorer clinical outcomes by a particular *TP53* mutation status.

Primary Readers:

Dr. Rachel Karchin,

Dr. Kymberleigh Pagel,

Dr. Brian Caffo

Acknowledgments

I am extremely grateful to my supervisor, Prof. Rachel Karchin, for accepting me in your lab and providing me with the opportunity to work on this fascinating project. Your support and care are valuable and necessary for my success as a master student.

I want to express my deepest gratitude to Dr. Kymberleigh Pagel, for mentoring me and helping me draft and edit this master thesis. The completion of this thesis would not have been possible without your contribution and advice.

I would also like to express my sincere appreciation to Prof. Brian Caffo, for kindly sparing time reading this thesis and giving me your precious feedback.

Special thanks to my families for their love and care!

The results shown here are in whole or part based upon data generated by the TCGA Research Network: https://www.cancer.gov/tcga.

Table of Contents

List of Tables

List of Figures

Chapter 1

Introduction and Background

Head and neck squamous cell carcinoma (HNSCC) is one of the six most common cancers worldwide, with over 80,000 people diagnosed with it in 2018 (Johnson, 2020). HNSCC could originate from multiple primary tumor sites: oral cavity, oropharynx, larynx and hypopharynx. The main risk factors for HNSCC include tobacco, alcohol and human papillomavirus (HPV) infection. The two subtypes of HNSCC, regarding the HPV status, HPV-associated (HPV+) and HPV-unassociated (HPV-), are clinically distinct, differing in both pathophysiology and prognosis. These differences at least partially driven by mutational patterns. While it is rare in HPV+ HNSCC, *TP53* is one of the most commonly altered genes in HPV- HNSCC, occurring in nearly all cases (Network, 2015). As with many other types of cancer, *TP53* mutation is an independent poor prognosis factor in HNSCC (Johnson, 2020). As a well-known tumor suppressor protein, p53 contributes significantly to counteract the tumor progression. For example, overexpression of p63 is observed to be related to HNSCC tumor, while normally functioning p53 would degrade p63 and therefore suppress HNSCC tumor (Partridge M, 2007). Mutated *TP53*

with altered function would lead to the dysregulation of its related pathways, including p53-mediated cell sentence and metabolism. Studies have also shown that HNSCC patients with mutated *TP53* tend to lose the sensitivity to response to chemotherapy treatments (Rodriguez-Ramirez C, 2018). If *TP53* mutations are present, about half of patients with locally advanced tumor and nearly all patients with tumor metastasis would die from their disease.

Similar to other malignancies, targeting the p53 pathway has remained a challenge due to the various roles that p53 plays in cellular function, and the presence of both gain and loss of function mutations (Muller and Vousden., 2014). Activated by cell stress, p53 functions as the key gene in cell-apoptosis, DNA damage repair, cell cycle regulation and differentiation (Zhou G, 2016). Recent research on the immunomodulatory effects of p53 suggested that p53 mutants modify tumor microenvironment (TME), contributing to immune escape. In HNSCC, *TP53*-mutated tumors have been shown to harbor significantly lower antitumor immune signature levels than wild type *TP53* tumors (Li L, 2020). As an analogy to macroscopic ecosystem, TME refers to the surrounding of tumor cells that is shaped by tumor cells and in favor of tumorigenesis, consisting of their neighboring cells, blood vessels and extracellular matrix, etc. (B., 2019). TME is essential for the development and metastasis of tumor. Here, I assessed the impact of tumor cells on TME via the infiltration of immune cells, also known as leukocytes. The abundance of immune infiltrates in HNSCC patients have established utility in patient stratification for improved assessment of prognosis and treatments, serving as potential targets and predictors (Hollern DP, 2019; Wu T, 2017).

Leukocytes are white blood cells including neutrophils, monocytes, eosinophils, basophils, and lymphocytes (Carrick JB, 2008). Monocytes can further differentiate into M0 macrophages and dendrite cells, and lymphocytes are regarded as the combination of B cells, T cells and NK cells. Resting M0 macrophages would polarize to tumor-promoting M2 macrophages, induced by IL-4, IL-13 and IL-10, while IFN-y and LPS would drive the polarization towards the path to tumor-suppressing M1 macrophages (Orekhov AN, 2019; Viola A, 2019). Mature T cells could be categorized by their cell surface markers: CD8 T cells, the cytotoxic T cells that fight against pathogen and malign cells like tumor cells directly, and CD4 T cells, the helper T cells that regulate immune response (Kishton RJ, 2017). The activation and differentiation of B cells into memory B cells and plasma cells require the assistance from CD4 T cells, particularly depending on the T follicular helper (Tfh) cells in germinal center (Kennedy R, 2019). Tfh cells also produce cytokines like IL-21 to modulate B cell proliferation (Cyster JG, 2019). Activated memory B cells and plasma cells are recognized to be crucial for anti-tumor immunity via secreting immunoglobulin and enhancing T cell response (Tokunaga R, 2019). Immune-related pathways such as NF-kB and MAPK activation, PI3K/Akt/mTOR pathway and IFN signaling also exert profound impact on the modification of TME, participating in the interaction networks of immune cells and regulating their abundance and activities (Wu T, 2017; Rothenberger NJ, 2018) .

In this work, I characterized the possible mechanisms by which *TP53* alterations impacted the generation of an immunosuppressive TME in HPV-

HNSCC. Existing paired whole exome sequencing (n=523) and RNA sequencing (n=501) data from TCGA-HNSC were analyzed using computational approaches to identify the immune infiltrates and clinical outcomes that were related to defective *TP53*. HPV- HNSCC patients with homozygous *TP53* mutation were found to be more likely to exhibit immunosuppressive TME and poorer survival status. I also identified *PIK3CA* mutation as a co-factor that could exaggerate this unfavorable situation, and highlighted key immune-related pathways that were downregulated in these patients. Immune infiltrates such as higher M0 macrophages and lower Tfh cells were recognized as indicators to reflect the status of TME for individual HNSCC patients.

Chapter 2

Methods and Materials

This study used patient data from Head and Neck Squamous Cell Carcinoma Cancer Genome Atlas (TCGA-HNSC) Project (Tomczak K, 2015). This dataset was examined from several aspects: HPV status, somatic mutation, copy number variation, allele zygosity, immune cell infiltration, and gene expression. To serve this aim, I first filtered out patients without record of these data points. After this step, 470 patients remained. Patients' HPV status was determined using a threshold of 10 for HPV NRPM, the normalized reads per million (Thorsson V, 2019). This value was obtained by multiplying the number of reads that hit the HPV viral genome of a sample with 10^6 and then dividing this result by the number of total reads of that sample. In further analysis, I retained only patients that were HPV-, which resulted in 406 samples.

***TP53* mutational status**

Somatic mutation calls for patients with HNSCC were obtained from Multi-Center Mutation Calling in Multiple Cancers (MC3, v0.2.8) (Ellrott K, 2018). On recommendations from the MC3 group, variants for which the FILTER

column did not equal "PASS" were excluded. Samples that were designated as hypermutators were also excluded. Based on the number of mutations found in the sample, hypermutators were defined as samples with greater than 1000 mutations, and with mutation count greater than 1.5 times the interquartile range above the third quartile of HNSCC patients. I further filtered out 82 patients with more than one mutation or silent mutations. Thus, remaining patients could be categorized into the following *TP53* status: wild type, missense, frame shift, in frame mutation, splice site or nonsense. I further separated missense mutation into two subcategories: gain-of-function (GOF) mutations (Muller and Vousden., 2014) and missense, and combined nonsense, frame shift and splice site mutation as loss-of-function (LOF) mutation.

***TP53* copy number alterations**

TP53 status could also be categorized from allele and copy number aspect: wild type, homozygous mutation, heterozygous mutation and mutation with a copy loss. The gene copy number scores were generated via GISTIC2 (Mermel et al., 2011) and retrieved from cBioPortal (Gao et al., 2013). The threshold values of GISTIC2 outputs were applied here, where 0 indicates no copy loss, -1 indicates shallow copy loss, while -2 indicates possibly a homozygous deletion. I obtained the allele information, the counts of reference alleles and alternative alleles, from the MC3 Mutation Annotation Format (MAF) file (Ellrott K, 2018). The variant allele frequency (VAF) was calculated based on this information and further normalized by tumor purity (Donehower LA, 2019). *TP53* mutation zygosity was determined by these normalized VAF values, where VAF

> 0.75 was regarded as a homozygous mutation, and otherwise heterozygous (Donehower LA, 2019). Patients were further divided into subgroups based upon their *TP53* mutation type: homozygous wildtype ($TP53^{wt/wt}$), patients with one or more copies of mutant *TP53*: heterozygous mutation, ($TP53^{wt/mt}$) or homozygous mutation, ($TP53^{mt/mt}$), and those with copy loss ($TP53^{mt/null}$). The combination of $TP53^{mt/mt}$ and $TP53^{mt/null}$ could also be regarded as loss-of-heterozygosity mutation ($TP53^{LOH}$). The $TP53^{wt/null}$ and $TP53^{null/null}$ groups were not considered in this study due to their significantly lower sample spaces (n=9/n=3). I also excluded samples with copy number amplification as there was not a well-defined criterion to evaluate their allele zygosity (n=40). Table 2.1 shows the distribution of *TP53*-mutated HNSCC HPV- patients, while 66/271 patients are in $TP53^{wt/wt}$ group.

	$TP53^{wt/mt}$	$TP53^{mt/mt}$	$TP53^{mt/null}$
Missense	11	27	33
LOF	18	37	25
GOF	9	22	18

Table 2.1: *TP53*-mutated HPV- HNSCC patient distribution

Immune cellular fractions

To contrast the relative fraction of immune cell types within the leukocyte compartment, I utilized immune cellular fractions and estimated aggregations from Thorsson et al (Thorsson V, 2019). These data were generated via CIBERSORT, using the default LM22 signature genes file to determine infiltrates of 22 immune cell subtypes including T cells, B cells and myeloid cells, etc. (Newman et al., 2015). Gene expression profiles of HNSCC patients

generated from RNA seq data were used as inputs for CIBERSORT. The ratios of immune cell subtypes were also taken into consideration to compare the relative abundance of these infiltrates among patients: M0 macrophages to total lymphocytes (M0/Lym). An outlier was removed with the M0/Lym ratio larger than 5. These immune cell abundances and their ratios were categorized as high or low relative to the mean value. Table 2.2 shows these thresholds. I excluded immune cell types whose infiltrate values that are missing in more than one third (90) of the patients. Statistical tests were used to contrast immune cell infiltrates among HPV- HNSCC patients with different *TP53* mutation status.

Cell Type	Threshold
Macrophage M0	0.155
T follicular helper cell	0.061
M0 / Lymphocytes	0.511

Table 2.2: Mean values of cell infiltrates

Gene expression Analysis

HTSeq-counts from RNA sequencing data were acquired from the Genomic Data Commons portal (Grossman, 2016). Genes were mapped from Ensembl identifier to their HUGO gene symbol using the GENCODE human genome (GRCh38, v22) (Frankish A, 2019). To avoid ambiguity, I filtered out 399 genes with more than one Ensembl identifier. To remove genes with low expression, genes with zero count in more than one third patients (n=90) were excluded. After this filtering, 32736 out of 60483 genes were left to differential gene expression analysis using DESeq2, where $TP53^{wt/wt}$ patients served as the

control group (Love MI, 2014). Genes with adjusted p-value less than 0.05 in the differential gene expression (DEG) analysis were used for downstream pathway enrichment analysis with Gene Set Enrichment Analysis (GSEA) (Subramanian A, 2005). The log-fold change scores of these genes after approximate posterior estimation for GLM coefficients shrinkage were used as enrichment scores (Zhu A, 2019). I used the Reactome (Fabregat A, 2017) and Hallmark pathways (Liberzon A, 2015) in the GSEA Pre-ranked analysis, with permutation number set to 1000 and a significance cutoff for false discovery rate (FDR) at less than 0.05. The top 25 pathways with higher enrichment scores from each *TP53* mutated group were selected for further investigation. DEG and GSEA analysis were also applied to contrast gene expressions and pathway regulations in tumor site and those in normal tissue within patients with same *TP53* status, following the above workflow.

Gene Co-Mutation Analysis

To detect genes whose mutations frequently co-occur with a certain subtype of *TP53* mutation, two methods were applied: first, I generated a list of genes that mutated in more than 15% samples for each *TP53* mutated group list one. Then, I inputted the gene mutation information of HNSCC HPV- patients into pairwise Multivariate Organization of Combinatorial Alterations (MOCA) analysis (Masica DL, 2011) to achieve a list of genes that mutated more frequently in this *TP53* mutated group compared to all other samples with FDR less than 0.05 and positive predictive value (PPV) more than 0.1, as list two. The union of genes in list one and list two were the genes of interest here and were examined for their association with survival status and tumor

microenvironment (TME). Thirteen genes were found for our group of interest, the $TP53^{mt/mt}$ group.

Survival Analysis

Survival analysis was applied to examine the impact of *TP53* gene alteration, cell infiltrates, and the co-occurrence of *TP53* mutation and mutation of other genes on the prognosis of HNSCC HPV- patients via the python package lifelines, using Kaplan-Meier estimator. The survival variables were extracted from cBioPortal for the TCGA-HNSC PanCancer dataset, specifically the OS_MONTHS and OS_STATUS variables for overall survival: decreased or alive; DSS_MONTHS and DSS_STATUS variables for disease-specific survival: alive or dead without tumor, dead from tumor (Tomczak K, 2015). I compared the survival curves between $TP53^{wt/wt}$ group and patients with mutated *TP53* subtypes, or patients with co-occurrence of mutated *TP53* subtypes and the mutation of some other gene. The association between cell infiltrates and patient survival was assessed via two aspects. Firstly, the survival curves between patient with high cell infiltrates and patient with low cell infiltrates were compared via statistical tests, using previously defined threshold. Secondly, patients were divided into two groups by their survival status: patients who decreased within two years and patients who survived for at least two years in order to check if any cell infiltrates or ratios was significantly different between these two groups.

Chapter 3

Results

HPV- HNSCC distinguished with poor survival status, unfavorable tumor microenvironment and more frequent *TP53* mutation

Overall survival analysis demonstrated that HPV- HNSCC patients had significantly poorer survival rate compared to the HPV+ patients (Log-rank test, p-value < 0.005, Figure 3.1 a). The tumor microenvironment (TME) among HPV- HNSCC patients showed differences in tumor cell infiltration, exhibiting significantly greater cell infiltration of macrophages and lower cell infiltration of lymphocytes (Mann-Whitney U test, p-value = 1.06e-12 and 4.58e-15 respectively, Figure 3.1 c-d), where decreased lymphocytes are known to associate with the suppression of anti-tumor immune response (Yang L, 2019) and tumor-associated macrophages promote an immunosuppressive TME (Lin Y, 2019). In addition, protein-coding *TP53* mutations were 50 times more frequent in HPV- HNSCC patients compared to the HPV+ HNSCC patients (330/406 HPV-, 1/64 HPV+). I then evaluated the relationships between the poor survival outcomes and specific subcategories of *TP53* mutations in HPV-

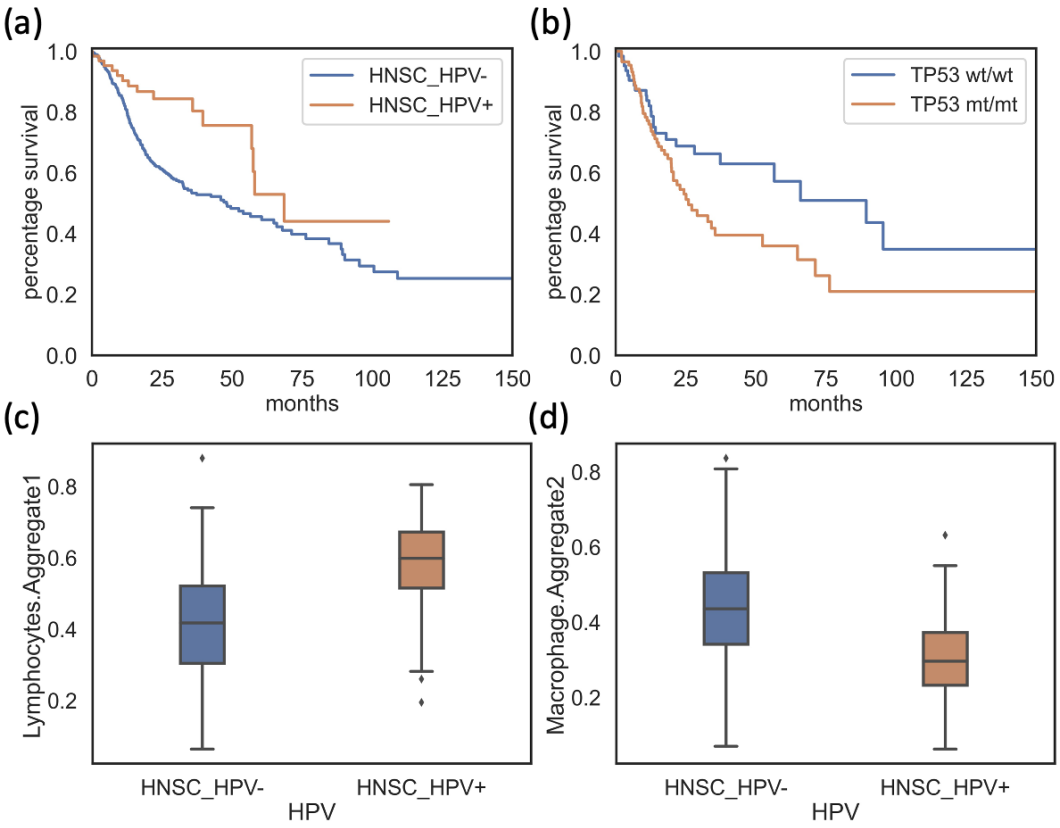

Figure 3.1: Plot contrasting survival status (a), lymphocytes infiltrates (c) and macrophages infiltrates (d) between HPV+ (orange) and HPV- (blue) patients from TCGA-HNSC. Plot contrasting survival status between homozygous *TP53* mutated patients ($TP53^{mt/mt}$, orange) and Wild Type *TP53* patients ($TP53^{wt/wt}$, blue) in HNSCC HPV- group (b).

HNSCC patients. Survival analysis showed a significantly lower survival rate in $TP53^{mt/mt}$ patients compared to $TP53^{wt/wt}$ patients (Figure 3.1 b, p-value=0.04). In the following sections, I sought to establish the joint effects of immune infiltrates and *TP53* alterations on the prognosis of HNSCC HPV- patients, and identify associations between *TP53* mutation and altered TME.

HPV- HNSCC patients with homozygous *TP53* mutation exhibited low T follicular helper cell and high M0 macrophage cell infiltration, which correlated with poor survival.

Since HNSCC is an immune-rich disease, the abundances of immune cells in TME may serve as indicators for patient survival and prognosis, and provide insights into how the tumor could impact TME. Evaluating the dissimilarity of pro-inflammatory and anti-inflammatory immune cell infiltrates among patients with different *TP53* mutation subtypes could also help to explain their distinct immune status. Therefore, I turned to find the association between immune cell infiltration and patient survival. In patients with poorer survival, significantly lower T follicular helper (Tfh) cells and higher M0 macrophages to aggregated lymphocytes ratio, M0/Lym, were observed (Mann-Whitney U test, p-value =4.44e-5 and 0.0035, respectively, Figure 3.2 a-b). Consistent with previous research (Wondergem NE, 2020; Gu-Trantien C, 2013; Thorsson V, 2019), overall survival analysis showed that lower Tfh cell infiltrate significantly related to poorer survival rate (Log rank test, p-value < 0.005, Figure 3.2 c). This negative impact of low Tfh cell infiltration could be explained by its irreplaceable role in the survival, maturation of B cells and T-cell-B-cell interaction (Lechner A, 2019; Hollern DP, 2019). Other studies suggested that higher monocyte-to-lymphocyte ratio was unfavorable for patient survival (Hu RJ, 2018; Yang YT, 2018). Monocyte infiltrates were hardly detected in HNSCC HPV- patients, as 101/271 patients were found to have zero value. However, a similar ratio, M0/Lym, was identified, where M0 macrophages

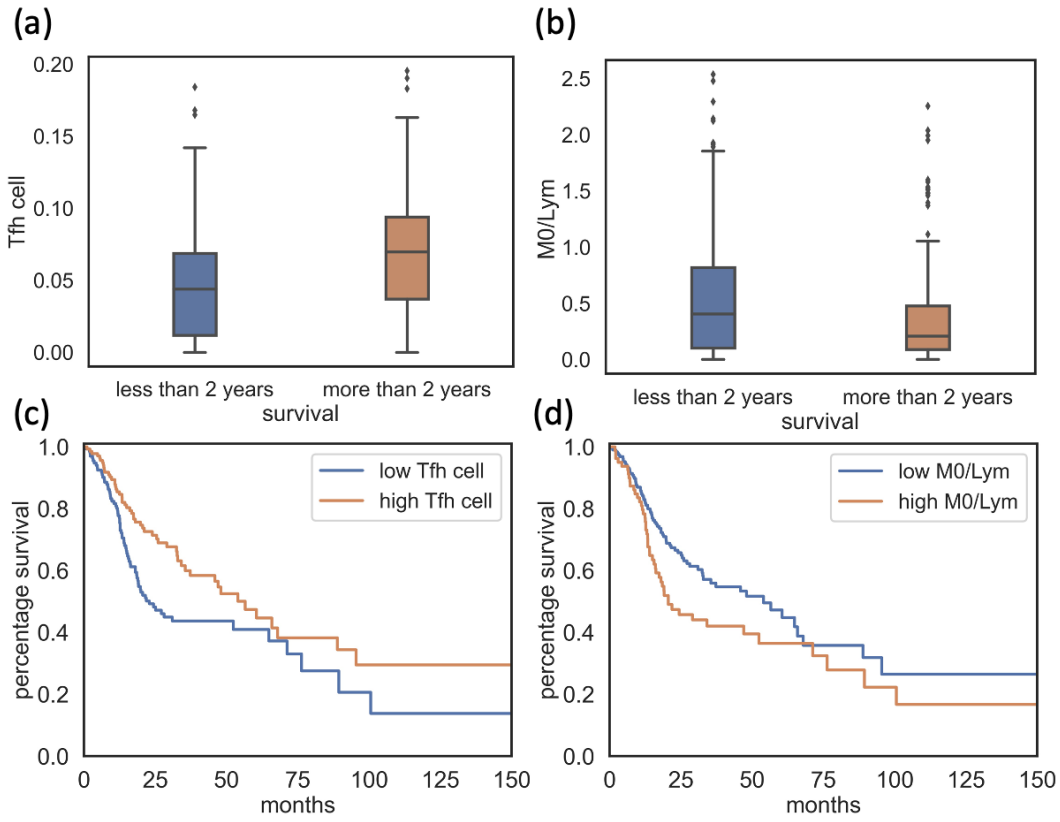

Figure 3.2: Plot contrasting differences in T follicular helper (Tfh) cell (a) and high M0 macrophage /Lymphocyte (M0/Lym) (b) in HPV- HNSCC patient group and the survival rate of patients with different Tfh cell (c) and M0/Lym ratio (d). Tfh cell = T follicular helper cell, M0 = M0 Macrophages, Lym = Aggregated lymphocytes

differentiated from monocytes and could polarize to pro-inflammatory M1 macrophages and anti-inflammatory M2 macrophages. A higher M0/Lym ratio was associated with poorer survival (Log rank test, p-value = 0.03, Figure 3.2 d).

With Tfh cell infiltration and M0/Lym ratio identified, I then went to see if these infiltration values were significantly different in the mutated *TP53* groups compared to wild type *TP53* patients. Significantly lower Tfh cell

infiltrates were found in the *TP53*$^{mt/mt}$ group (Mann-Whitney U test, p-value = 0.026, Figure 3.3 a). Patients in the *TP53*$^{mt/mt}$ group and the *TP53*$^{mt/null}$ group also had significantly higher M0/Lym (Mann-Whitney U test, p-value = 0.004 and 0.0004 respectively, Figure 3.3 b). A strong negative correlation between M0 macrophages and lymphocyte infiltrates was found (Pearson correlation, coefficient = -0.66, p-value = 1.52e-34, Figure 3.3 c). Considering that the lymphocytes are consisted of multiple disparate cells, M0 macrophages were used to represent M0/Lym ratio, while the impact of M0 macrophages was also supported by Jairath et al. (Jairath NK, 2020). The comparison of M0 macrophage infiltrates between different mutated *TP53* groups and wild type *TP53* group returned similar findings to that of M0/Lym, where the *TP53*$^{mt/mt}$ group and the *TP53*$^{mt/null}$ group stood out with significantly higher M0 macrophage infiltrates, supporting the usage of M0 macrophages to reflect M0/Lym ratio for simplicity (Mann-Whitney U test, p-value = 0.006 and 0.0007 respectively, Figure 3.3 d). I also observed significantly lower CD8 T cell infiltrates in *TP53*$^{mt/mt}$ patients and *TP53*$^{mt/null}$ patients (Mann-Whitney U test, p-value = 0.0001 and 6.99e-7 respectively), as well as lower pro-inflammatory M1 macrophage infiltrates (Mann-Whitney U test, p-value = 0.007 and 0.0006 respectively). Both of them were recognized as signs to indicate immunosuppressive TME (Padoan A, 2019; Choo YW, 2018). In combination, these immune cell infiltrates shaped the unfavorable TME of *TP53*$^{mt/mt}$ patients and *TP53*$^{mt/null}$ patients. However, distinctions between TME of *TP53*$^{wt/mt}$ patients and *TP53*$^{wt/wt}$ patients were not obvious.

The survival analysis could be further extended from overall survival (OS) to

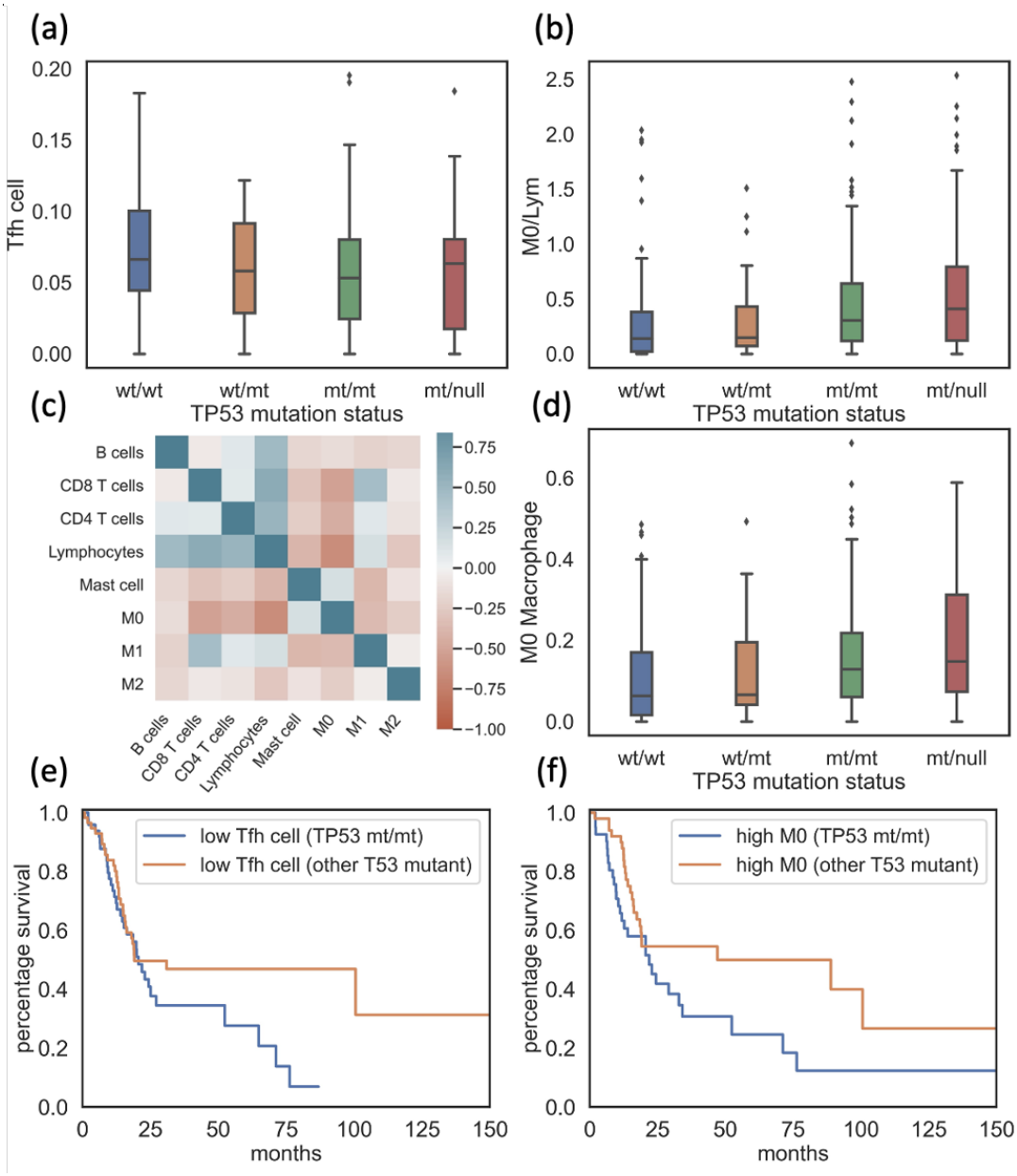

Figure 3.3: Plot contrasting the Tfh cell (a), M0/Lym ratio (b), and M0 infiltrates (c) in HNSCC HPV- patients with different *TP53* types. Heatmap representing Pearson correlation of immune cell infiltrates. (d) Overall survival curve for patients with low Tfh cell infiltrates (e) and high M0 macrophage infiltrates (f) contrasting $TP53^{mt/mt}$ group and group with other *TP53* mutations. Tfh cell = T follicular helper cell, M0 / Lym = M0 Macrophages over Aggregated lymphocytes.

disease-specific survival (DSS), where patients were categorized as (1) alive or dead without tumor or (2) dead from tumor rather than simply alive or decreased. This categorization could reduce the noise of other factors like age and the existence of other diseases in survival analysis. However, due to the relatively incomplete record of HPV- HNSCC patients' disease-specific survival status, here I applied this analysis as a validation method to ensure that our finding would still hold from another more stringent aspect. Similar as OS analysis, DSS analysis showed obviously poorer survival of the $TP53^{mt/mt}$ group compared to the $TP53^{wt/wt}$ group, and more noticeable difference between the survival status between the $TP53^{mt/mt}$ group and the $TP53^{mt/null}$ group (Log rank test, p-value = 0.07 and 0.67 respectively, Figure 3.4 (a)-(b)). The statement that patients with lower Tfh cell infiltrates or higher M0/Lym ratios have significantly more unfavorable survival continued to hold in DSS analysis, using the same threshold value as OS analysis (Log rank test, p-value = 0.03 and 0.02, respectively, Figure 3.4 (c)-(d)).

As discussed in previous section, the $TP53^{mt/mt}$ group showed a significantly poorer survival compared to the $TP53^{wt/wt}$ group, which might be explained at least partially, by this unfavorable TME pattern of this group. The $TP53^{mt/mt}$ group tended to have low Tfh cell and high M0 macrophage infiltrates, both of which were identified to significantly associated with poor prognosis. I then noticed that within the patients with low Tfh cell infiltrates and patients with high M0 macrophage infiltrates, homozygous *TP53* mutation also seemed to be the driving co-factor for the unfavorable survival, where in the survival

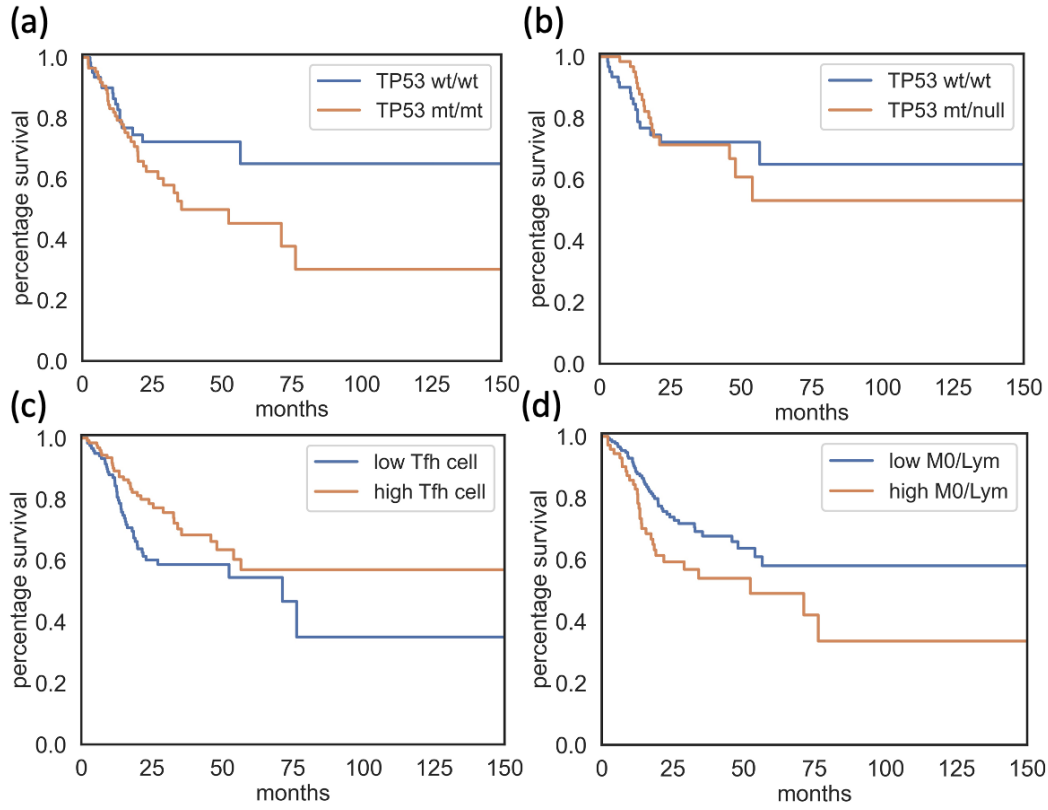

Figure 3.4: Plot contrasting survival status between $TP53^{mt/mt}$ patients (orange) (a) or $TP53^{mt/null}$ patients, orange (b) and $TP53^{wt/wt}$ patients (blue). Plot contrasting survival status between patients with low cell infiltrate (blue) and patients with higher cell infiltrate (orange) of Tfh cell (c) and M0/Lym ratio (d). Tfh cell: T follicular helper cell; M0/Lym: M0 macrophage over Aggregated lymphocytes ratio

analysis, patients with other *TP53* mutation status have better outcomes compared to $TP53^{mt/mt}$ patients (Log rank test, p-value = 0.06 and 0.02 respectively, Figure 3.3 e-f). Such differences in survival did not hold in other mutated *TP53* groups, implying some uniqueness of $TP53^{mt/mt}$ patients.

The immunosuppressive tumor microenvironment of $TP53^{mt/mt}$ patients co-occurs with down-regulation of immune-related gene interactions which differ from those of $TP5^{mt/null}$ patients.

Though $TP53^{mt/mt}$ patients bore significantly poorer survival rate, patients with $TP53^{LOH}$ mutations ($TP53^{mt/mt}$ and $TP53^{mt/null}$) shared the similar immunosuppressive TME. Gene expression and pathway regulation of these two groups were contrasted via DEG and GSEA analysis to find possible mechanisms explaining the difference. The expressions of *TP53* in patients with *TP53* mutations did not differ from $TP53^{wt/wt}$ patients. However, a significant decrease was detected in the expression of *TP53* inducible nuclear protein 1 (*TP53INP1*) and *TP53* inducible protein 3 (*PIG3*) in both $TP53^{LOH}$ groups, indicating the dysfunction of mutated *TP53*. Interestingly, $TP53^{mt/null}$ patients also showed an increase of the expression of *TP53* inducible protein 11 (PIG11), an *TP53*-activated gene which could suppress tumor metastasis by hindering the epithelial-mesenchymal transition and triggering p53-dependent cell apoptosis (Xiao T, 2019; Wang Y, 2018; Liu XM, 2009). This result suggests the possibility that $TP53^{mt/null}$ patients were having more "normally" functioning *TP53* compared to the $TP53^{mt/mt}$ group, and that alternative pathways were activated in the $TP53^{mt/null}$ group to regulate some of the *TP53*-dependent

tumor suppressor genes. The overexpression of this tumor suppressor protein might associate with the relatively better survival of *TP53*$^{mt/null}$ patients.

I further split *TP53*$^{mt/mt}$ patients and *TP53*$^{mt/null}$ patients by their *TP53* mutation subtypes from another aspect: GOF, LOF and missense. Significantly higher M0/Lym ratio was found in *TP53*$^{mt/mt}$ patients with LOF and missense mutations, as well as *TP53*$^{mt/null}$ patients with GOF and missense mutation. Lower Tfh cell infiltrates were found in *TP53*$^{mt/mt}$ and *TP53*$^{mt/null}$ patients with missense mutations. Overall survival analysis revealed that *TP53*$^{mt/mt}$ patients with missense and LOF mutations tended to have unfavorable survival, as well as *TP53*$^{mt/null}$ patients with GOF mutations (Log rank test, p-value = 0.04, 0.14 and 0.06 respectively). Such unfavorable survival also seemed to be associated with whether the mutated *TP53* could preserve the normal function, at least partially, since groups with poor survival tended to decreased expressions of *TP53* inducible proteins, while the expression of *TP53* inducible proteins of other mutated *TP53* groups were either overexpressed or did not differ from that of the *TP53*$^{wt/wt}$ group.

GSEA analysis further illustrated the distinctiveness among the most downregulated pathways of the *TP53*$^{mt/mt}$ group and the *TP53*$^{mt/null}$ group. Only 8 (32%) of the top 25 down-regulated pathways were commonly shared among these groups. The most downregulated pathways in the *TP53*$^{mt/mt}$ group included IL-10 synthesis, BCR signaling, and NF-kB and MAPK activation, while the *TP53*$^{mt/null}$ group presented major downregulation in IFN-y response, IFN signaling and TCR signaling, suggesting different mechanisms leading

to the immunosuppressive TME in these two groups. The most significantly down-regulated pathways found in $TP53^{mt/mt}$ patients also participated in macrophage activation and polarization, such as the FCERI mediated activation of MAPK and NF-kB activation, and the FCGR3A mediated IL-10 synthesis. Since IL-10 could promote the polarization towards M2 macrophages, down-regulation of IL-10 synthesis would directly inhibit M2 polarization (Viola A, 2019; Sun Y, 2020).

Macrophage activation could be also regulated by NF-kB and MAPK signaling (Nie Y, 2019; Park JI, 2019). The inhibition of these two pathways would result in the suppression of macrophage differentiation, especially towards the M1 macrophages direction (Sun Y, 2020; Islam SU, 2018). Downregulation of them in $TP53^{mt/mt}$ patients may also contribute to their significantly high M0 abundance, as a consequence of reduction in macrophage activation and polarization. Further considering the impact of Tfh cells on B lymphocytes, the low Tfh cell infiltrates might also relate to the high M0 macrophage infiltrates. B cells could induce the polarization of M2 macrophage via IL-10 signaling (Affara NI, 2014). Therefore, the suppression of B cell activation caused by the low Tfh cells could inhibit the polarization from macrophages M0 to M2. Significantly down-regulated IL-10 synthesis and B cell receptor (BCR) related pathways, for example, CD22 mediated BCR regulation and signaling by BCR, in the $TP53^{mt/mt}$ group supported this possibility. Besides mediating the activation of NF-kB and MAPK, FCERI (IgE receptor) itself could also contribute to the elevation of M0 macrophage infiltrates. IgE would

activate M0 macrophages via binding to its receptor, FCERI. Therefore, reduced FCERI could inhibit the polarization of M0 macrophage (Zhang X, 2020; Karagiannis SN, 2017). To summarize, these top down-regulated pathways together negatively regulated the activation and polarization of resting M0 macrophages towards either pro-inflammatory M1 or anti-inflammatory M2 direction, therefore leading to the immunosuppressive TME of $TP53^{mt/mt}$ patients.

The Co-occurrence of *PIK3CA* kinase region mutation in $TP53^{mt/mt}$ patients promotes the immunosuppressive TME and contributes to poor survival

The mutation of a single gene is unlikely to be the only driving factor to cancer development. I hypothesized that the co-occurrence of some additional factors, such as mutation of other genes, may together promote poor patient survival. Among genes of interest, the mutations of gene *PIK3CA* were found to be associated with poor prognosis, when co-occurring with homozygous *TP53* mutation (Log rank test, p-value = 0.02, Figure 3.5 a). This finding was supported by previously published studies, suggesting that the co-mutation of *TP53* and *PIK3CA* is related to poor clinical outcomes (Li AJ, 2018; Chen X, 2019). Studies have shown that *PIK3CA* mutations lead to a continuous activation of PI3K/Akt/mTOR pathway (Fujimoto Y, 2020; Zhang Y, 2017). The hyperactivation of PI3K/Akt/mTOR pathway has been observed in multiple cancer types and the inhibition of this pathway has been an option for cancer immunotherapy, due to its role in promoting cell proliferation, survival and migration (O'Donnell JS, 2018; Okkenhaug K, 2016). The PI3K/Akt/mTOR

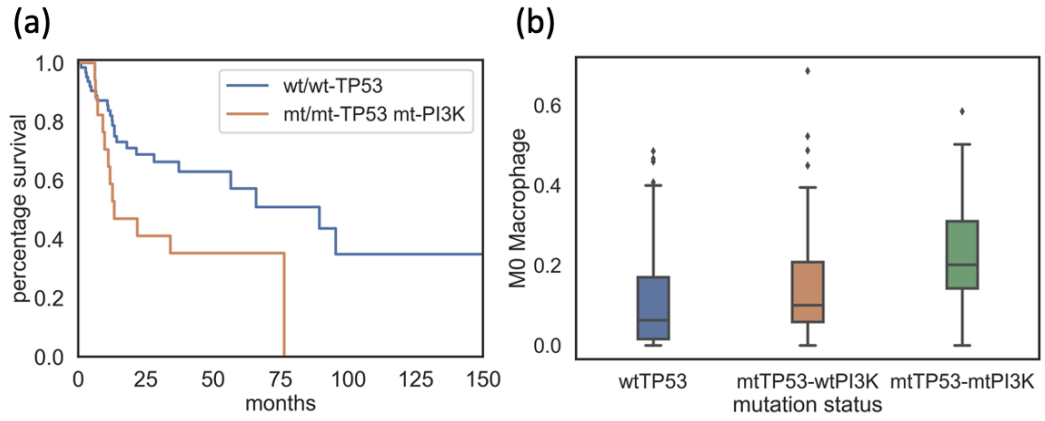

Figure 3.5: Plot contrasting the survival curve of wild type *TP53* patients and patients with both *TP53* and *PIK3CA* mutations (a). Plot contrasting M0 macrophage infiltrates of $TP53^{wt/wt}$ group, $TP53^{mt/mt}$ group with wild type *PIK3CA* and $TP53^{mt/mt}$ group with mutated *PIK3CA* (b).

pathway might also contribute to the immunosuppressive TME via its impact on the motility and polarization of macrophages.

Moreover, *PIK3CA* mutations in exon-20 and exon-9 kinase regions, which were the major type of *PIK3CA* mutations in our data set, have previously been shown to associate with up-regulation of phosphorylated Akt (p-Akt) expression (Sonnenblick A, 2019). Increased Akt activation leads to the reduction of macrophage polarization (Vergadi E, 2017). The overexpression of *PIK3CA* could also result in the elevation of macrophage infiltration (Xie S, 2014). Therefore, I postulated that the mutations of *PIK3CA* may contribute to the over-abundance of unpolarized M0 macrophage. This hypothesis was further supported by other work, which suggested that the upregulation of *PIK3CA* might contribute to the suppression of pro-inflammatory cytokines, and thus decrease the polarization to pro-inflammatory M1 macrophage (Xie S, 2014;

Viola A, 2019), which could lead to an over-abundance of M0 macrophage. As shown in Figure 3.5 (b), the M0 macrophage infiltration of *TP53*$^{mt/mt}$ patients with *PIK3CA* mutation was higher than both *TP53*$^{wt/wt}$ patients and *TP53*$^{mt/mt}$ patients with wild type *PIK3CA*.

I also observed a relatively lower *PIK3CA* mutation frequency, (9.09% (7/77) in the *TP53*$^{mt/null}$ group compared to 19.1% (17/89) in the *TP53*$^{mt/mt}$ group and 29.3% (12/41) in the *TP53*$^{mt/mt}$ group with a high M0 abundance. This difference may also count as an explanation for the poorer clinical outcome of *TP53*$^{mt/mt}$ group. Again, the enhancement of *PIK3CA* mutation frequency in the *TP53*$^{mt/mt}$ group with higher M0 abundance (19.1% to 29.3%) suggested the correlation of *PIK3CA* mutation and the suppression of macrophage polarization.

Chapter 4

Discussion and Conclusion

HPV- HNSCC patients with homozygous *TP53* mutation observed to have poorer survival and immunosuppressive TME

HNSCC tumors are among the most highly immune-infiltrated cancer types, and present an urgent challenge to identify more effective treatments. Increased *TP53* mutations are presented among HPV- cases compared to HPV+. These HPV- cases also exhibit poorer clinical outcomes and more immunosuppressive tumor microenvironment (TME). Characterization of HPV- HNSCC patients based upon *TP53* mutation types could be used to identify patients with poorer survival outcomes, and identify the major down-regulated immune pathways among these patients. In particular, patients with homozygous *TP53* mutation, $TP53^{mt/mt}$, exhibited poorer survival and more unfavorable immune infiltrate pattern: lower T follicular helper (Tfh) cell infiltrates and higher ratio of M0 macrophages over aggregated lymphocytes, which I used M0 macrophage infiltrate as a substitute. These two immune cell infiltrates, Tfh cells and M0 macrophages, were found to be correlated with poorer

patient survival. These aspects may together explain for the immunosuppressive TME of *TP53*$^{mt/mt}$, at least partially. The higher M0/Lym ratio and M0 macrophage infiltrates, as well as lower CD8 T cells and tumor-suppressing M1 macrophages, were also observed in *TP53*$^{mt/null}$ patients, establishing the similar unfavorable TME as *TP53*$^{mt/mt}$ patients.

Besides implying the lack of ability to polarize, high M0 macrophages could also be damaging to patients for their potential M2-like property as previous studies stated (Orekhov AN, 2019; Kumar AT, 2019; Jairath NK, 2020). Such anti-inflammatory trait of M0 macrophages could be detrimental to patients, when M2 macrophages infiltrates did not vary significantly among HPV- HNSCC groups with different *TP53* status. Low Tfh cell infiltrates would directly impact the maturation, activation and survival of B cells and therefore impact the anti-tumor immunity (S., 2014). Within patients with homozygous *TP53* mutation, those with co-occurrence of *PIK3CA* mutations in exon-9 and exon-20 kinase regions tended to have an exaggerated undesirable survival status. Studies have shown that *PIK3CA* mutations in these two kinase regions would lead to the increased phosphorylated Akt (p-Akt), which could inhibit the polarization of M0 macrophages to M1 macrophages (Vergadi E, 2017; Sonnenblick A, 2019). I noticed that these patients exhibited higher abundance of unpolarized M0 macrophages and significantly higher M0/Lym ratio, even compared to *TP53*$^{mt/mt}$ patients with wild type *PIK3CA* (Mann-Whitney U test, p-value =0.035).

The altered TME of *TP53*$^{mt/mt}$ patients could be impacted by the downregulation of immune-related pathways and *TP53* mutation

Several pathways among the most downregulated pathways of *TP53*$^{mt/mt}$ patients could correlate with the unfavorable TME: NF-kB and MAPK activation, IL-10 synthesis and B cell receptor (BCR) signaling. While the downregulation of NF-kB and MAPK activation, and IL-10 synthesis would reduce macrophage activation and polarization, suppressed BCR signaling and regulation might result from the decreased Tfh cell infiltrates. These impacted pathways may also associate with *TP53* mutations. Studies have suggested that *TP53* is involved in the activation and signaling of MAPK as a upstream regulator (GS., 2004; Gulati AP, 2006; Brown L, 2006). Dysfunctional *TP53* would potentially lead to the opposite direction and therefore result in the downregulation of MAPK activation. *TP53* would promote the synthesis and secretion of IL-10, which may count for the decrease of IL-10 synthesis in the *TP53*$^{mt/mt}$ group (Bueter M, 2006; Huang YH, 2020). Since normally functioned *TP53* induces the differentiation of M0 macrophages to pro-inflammatory M1 macrophages (Blagih J, 2020), mutant *TP53* would also inhibit the polarization towards this direction. The significantly decreased expressions of *TP53* directly induced proteins, such as PIG11 and PIG3, together indicated that mutant *TP53* in *TP53*$^{mt/mt}$ patients was malfunctioned.

However, most studies suggested that *TP53* inhibits NF-kB activation (Liu G, 2009; Murphy SH, 2011) and mutant *TP53* enhances the duration of NF-kB activation (Vaughan CA, 2012), indicating that there might be other causes for

the downregulation of NF-kB activation in the *TP53*$^{mt/mt}$ group. A potential cause might be the pathway interaction of NF-kB, MAPK and FCERI signaling (Zhang X, 2020; Schulze-Osthoff K, 1997). GSEA analysis also revealed the difference of the most downregulated pathways in *TP53*$^{mt/mt}$ patients and *TP53*$^{mt/null}$ patients. Instead of MAPK activation, BCR signaling and IL-10 synthesis, *TP53*$^{mt/null}$ patients were identified with reduced IFN-y response, and T cell receptor (TCR) and IFN signaling. The downregulation of these pathways could contribute to the high M0 macrophage infiltration of *TP53*$^{mt/null}$ patients. Recent studies suggested the involvement of interferon, including IFN-y in macrophage activation (Pascarella A, 2021; Huangfu N, 2020). While downregulation of TCR-related pathways, for example, TCR signaling and phosphorylation of CD3 and TCR zeta chain, were significant markers for dysfunctional T cells and immunosuppressive TME, such downregulation might associate with the increased abundance of M0 macrophage infiltration (Sikora J, 2004; Ezernitchi AV, 2006). I also observed enhanced expression of *TP53*-induced protein in *TP53* in *TP53*$^{mt/null}$ patients, suggesting the possibility that *TP53* in *TP53*$^{mt/null}$ patients could bear more "normally functioned" *TP53* or *TP53* substitute compared to *TP53* in *TP53*$^{mt/mt}$ patients.

A limited portion of tumor site RNA seq data from GDC portal were paired with corresponding normal tissue RNA seq data: 7 *TP53*$^{wt/wt}$ patients, 4 *TP53*$^{wt/mt}$ patients, 16 *TP53*$^{mt/mt}$ patients and 7 *TP53*$^{mt/null}$ patients. Due to the incomplete sample space, it was hard to draw conclusion from these data. However, gene expression analysis might provide a hint of possible gene activity alterations in tumor sites compared to normal tissues of patients

with different *TP53* mutation status. No significantly altered pathways were observed in the $TP53^{wt/mt}$ group. Several cell-cycle related pathways were found to be enhanced in this group, such as G2M checkpoint, mitotic G1 phase and G1/S transition, E2F targets and DNA synthesis, while no typical downregulated pathways detected in $TP53^{wt/wt}$ patients (Kent, 2019). Similarly, there were no noticeable pathway downregulation in $TP53^{mt/null}$ group. However, I observed that almost all downregulated pathways found in $TP53^{mt/mt}$ patients relative to $TP53^{wt/wt}$ patients were significantly enriched in the $TP53^{mt/mt}$ group, tumor site compared to normal tissue: FCERI-mediated NF-kB and MAPK activation, IL-10 synthesis and BCR signaling. Again, considering the small sample size (4 patients), the observation could only serve as a reference, at most. Besides the hyperactivation of cell cycle modulating pathways, $TP53^{mt/mt}$ patients also showed remarkable upregulation of epithelial mesenchymal transition (EMT) related pathways, for example, epithelial mesenchymal transition and extracellular matrix proteoglycans. EMT is an essential step for tumor metastasis (Scott LE, 2019). Such upregulation in $TP53^{mt/mt}$ patients could aggregate tumor progression and make patients more vulnerable, for high enrichment of EMT relevant pathways were not observed in patients from other groups.

The limitation and possible future direction of this study

This study could be limited, with multiple possible aspects for further investigation. It basically is a re-analysis of existing data and most of the data originated from bulk RNA and DNA sequencing data. The application of

bulk sequencing data alone would possibly affect the accuracy and specificity, compared to single cell sequencing data. Moreover, gene expression data generated from RNA seq count do not necessarily represent the actual protein expression level, and protein level might not equal to functioning protein level. For example, the phosphorylation of Akt is required for activation and downstream signaling (Sonnenblick A, 2019). However, whether proteins are phosphorylated or not could not be induced from RNA sequencing data. Another aspect of this study which is worth noticing is that cell infiltration values used were direct output of CIBERSORT (Newman et al., 2015), which was the relative abundance in the context of leukocytes (Thorsson V, 2019). Upon consideration of the complicated gene and pathway interactions in immune system, the immunosuppressive TME and altered pathways are unlikely to have only a single cause. For example, the high M0 macrophage infiltration could be affected by pathways other than NF-kB and MAPK activation, etc. Without supportive evidence from wet lab experiments, it is also hard to identify *TP53* mutation as the major cause of the downregulation of these pathways.

Through the GSEA and DEG analysis, I was able to observe the differences in major downregulated pathways and the expressions of *TP53*-dependent tumor suppressor genes in the $TP53^{mt/mt}$ group and the $TP53^{mt/null}$ group. However, further investigation is needed to fully unravel the intrinsic distinction of $TP53^{mt/mt}$ patients compared to $TP53^{mt/null}$ patients. $TP53^{mt/null}$ patients have a similar TME as $TP53^{mt/mt}$ patients and even more significantly deferentially expressed gene sets when compared to wild type *TP53* patients

(4745 genes for the *TP53*$^{mt/mt}$ group; 7760 genes for the *TP53*$^{mt/null}$ group, DESeq2 output). However, *TP53*$^{mt/mt}$ patients are the group with unfavorable survival, whereas the *TP53*$^{mt/null}$ patients shared a similar survival curve with wild type *TP53* patient in disease-specific survival analysis (Figure 3.1 (b)). The previous section mentioned that signatures for M2 macrophages could also be observed in M0 macrophages. Considering that polarized macrophages could be categorized into several subtypes: M2a, M2b, M2c and M2d (Viola A, 2019), it could also be possible to identify a specific subtype of M0 macrophages, probably with M2-like characteristic, which could be more anti-inflammatory and contribute to tumor progression. If such situation exists, it might be an explanation for the different survival status of *TP53*$^{mt/mt}$ and *TP53*$^{mt/null}$ patients, given their similar higher overall M0 macrophages.

Though this study focused on HPV- HNSCC, *TP53* mutations are prevalent in other cancer types, and so these findings may be more broadly applicable. Preliminary work has shown promise in the application of particular immunotherapeutic approaches. I hope that these insights can be used to improve survival outcomes among these more vulnerable patients.

References

Johnson D.E., Burtness B. Leemans C.R. et al. (2020). "Head and neck squamous cell carcinoma." In: *Nat Rev Dis Primers.* 6.1, p. 92.

Network, Cancer Genome Atlas (2015). "Comprehensive genomic characterization of head and neck squamous cell carcinomas." In: *Nature.* 517.7536, pp. 576–582.

Partridge M Costea DE, Huang X. (2007). "The changing face of p53 in head and neck cancer." In: *Int J Oral Maxillofac Surg.* 36.12, pp. 1123–1138.

Rodriguez-Ramirez C, Nör JE. (2018). "p53 and Cell Fate: Sensitizing Head and Neck Cancer Stem Cells to Chemotherapy." In: *Crit Rev Oncog.* 23.3-4, pp. 173–187.

Muller, Patricia A J and Karen H Vousden. (2014). "Mutant p53 in cancer: new functions and therapeutic opportunities." In: *Cancer cell.* 25.3, pp. 304–317.

Zhou G Liu Z, Myers (2016). "TP53 Mutations in Head and Neck Squamous Cell Carcinoma and Their Impact on Disease Progression and Treatment Response." In: *J Cell Biochem JN.* 117.12, pp. 2682–2692.

Li L Li M, Wang X. (2020). "Cancer type-dependent correlations between TP53 mutations and antitumor immunity." In: *DNA Repair (Amst).* 88.102785, pp. –.

B., Arneth (2019). "Tumor Microenvironment." In: *Medicina (Kaunas).* 56.1, p. 15.

Hollern DP Xu N, Thennavan A Glodowski C Garcia-Recio S Mott KR He X Garay JP Carey-Ewend K Marron D-Ford J Liu S Vick SC Martin M Parker JS Vincent BG Serody JS Perou CM. (2019). "B Cells and T Follicular Helper Cells Mediate Response to Checkpoint Inhibitors in High Mutation Burden Mouse Models of Breast Cancer." In: *Cell.* 179.5, pp. 1191–1206.

Wu T, Dai Y. (2017). "Tumor microenvironment and therapeutic response." In: *Cancer Lett.* 387.1, pp. 61–68.

Carrick JB, Begg AP. (2008). "Peripheral blood leukocytes." In: *Vet Clin North Am Equine Pract.* 24.2, pp. 239–259.

Orekhov AN Orekhova VA, Nikiforov NG Myasoedova VA Grechko AV Romanenko EB Zhang D Chistiakov DA. (2019). "Monocyte differentiation and macrophage polarization." In: *Vessel Plus* 3.1, p. 10.

Viola A Munari F, Sánchez-Rodríguez R Scolaro T Castegna A. (2019). "The Metabolic Signature of Macrophage Responses." In: *Front Immunol.* 10.1, p. 1462.

Kishton RJ Sukumar M, Restifo NP. (2017). "Metabolic Regulation of T Cell Longevity and Function in Tumor Immunotherapy." In: *Cell Metab.* 26.1, pp. 94–6109.

Kennedy R, Klein U. (2019). "A T Cell-B Cell Tumor-Suppressive Axis in the Germinal Center." In: *Immunity.* 51.2, pp. 204–206.

Cyster JG, Allen CDC. (2019). "B Cell Responses: Cell Interaction Dynamics and Decisions." In: *Cell.* 177.3, pp. 524–6560.

Tokunaga R Naseem M, Lo JH Battaglin F Soni S Puccini A Berger MD Zhang W Baba H-Lenz HJ. (2019). "B cell and B cell-related pathways for novel cancer treatments." In: *Cancer Treat Rev.* 73.1, pp. 10–19.

Rothenberger NJ Somasundaram A, Stabile LP. (2018). "The Role of the Estrogen Pathway in the Tumor Microenvironment." In: *Int J Mol Sci.* 19.2, p. 611.

Tomczak K Czerwińska P, Wiznerowicz M. (2015). "The Cancer Genome Atlas (TCGA): an immeasurable source of knowledge." In: *Contemp Oncol (Pozn).* 19.1A, A68–A77.

Thorsson V Gibbs DL, Brown SD Wolf D Bortone DS Ou Yang TH Porta-Pardo E Gao GF-Plaisier CL Eddy JA-Ziv E Culhane AC Paull EO Sivakumar IKA Gentles AJ Malhotra R Farshidfar F Colaprico A Parker JS Mose LE Vo NS Liu J Liu Y Rader J Dhankani V Reynolds SM Bowlby R Califano A Cherniack AD Anastassiou D Bedognetti D Mokrab Y Newman AM Rao A Chen K Krasnitz A Hu H Malta TM Noushmehr H Pedamallu CS Bullman S-Ojesina AI Lamb A Zhou W Shen H Choueiri TK Weinstein JN Guinney J Saltz J Holt RA Rabkin CS; Cancer Genome Atlas Research Network Lazar AJ Serody JS Demicco EG Disis ML Vincent BG Shmulevich I. (2019). "The Immune Landscape of Cancer." In: *Immunity.* 51.2, pp. 411–412.

Ellrott K Bailey MH, Saksena G Covington KR Kandoth C Stewart C Hess J-Ma S Chiotti KE-McLellan M Sofia HJ-Hutter C Getz G Wheeler D Ding L. (2018). "Scalable Open Science Approach for Mutation Calling of Tumor Exomes Using Multiple Genomic Pipelines." In: *Cell Syst.* 6.3, pp. 271–281.

Mermel, Craig H., Steven E. Schumacher, Barbara Hill, Matthew L. Meyerson, Rameen Beroukhim, and Gad. Getz (2011). "GISTIC2.0 facilitates sensitive

and confident localization of the targets of focal somatic copy-number alteration in human cancers." In: *Genome Biology.* 12.4, R41.

Gao, Jianjiong, Bülent Arman Aksoy, Ugur Dogrusoz, Gideon Dresdner, Benjamin Gross, S. Onur Sumer, Yichao Sun, Anders Jacobsen, Rileen Sinha, Erik Larsson, Ethan Cerami, Chris Sander, and Nikolaus Schultz (2013). "Integrative Analysis of Complex Cancer Genomics and Clinical Profiles Using the cBioPortal." In: *Science Signaling.* 6.269, pl1.

Donehower LA Soussi T, Korkut A Liu Y Schultz A Cardenas M Li X-Babur O Hsu TK-Lichtarge O Weinstein JN-Akbani R Wheeler DA. (2019). "Integrated Analysis of TP53 Gene and Pathway Alterations in The Cancer Genome Atlas." In: *Cell Rep.* 28.5, pp. 1370–1384.

Newman, Aaron M, Chih Long Liu, Michael R Green, Andrew J Gentles, Weiguo Feng, Yue Xu, Chuong D Hoang, Maximilian Diehn, and Ash A. Alizadeh (2015). "Robust enumeration of cell subsets from tissue expression profiles". In: *Nature Methods.* 12.5, pp. 453–457.

Grossman Robert L., Heath Allison P. Ferretti Vincent Varmus Harold E. Lowy Douglas R.-Kibbe Warren A. Staudt-Louis M. (2016). "Toward a Shared Vision for Cancer Genomic Data." In: *New England Journal of Medicine.* 375.12, pp. 1109–1112.

Frankish A Diekhans M, Ferreira AM Johnson R Jungreis I Loveland J Mudge JM-Sisu C Wright J-Armstrong J Barnes I-Berry A Bignell A Carbonell Sala S Chrast J Cunningham F Di Domenico T Donaldson S Fiddes IT García Girón C Gonzalez JM Grego T Hardy M Hourlier T Hunt T Izuogu OG Lagarde J Martin FJ Martínez L Mohanan S Muir P Navarro FCP Parker A Pei B Pozo F Ruffier M Schmitt BM Stapleton E Suner MM Sycheva I Uszczynska-Ratajczak B Xu J Yates A Zerbino D Zhang Y Aken B Choudhary JS Gerstein M Guigó R Hubbard TJP Kellis M Paten B Reymond A Tress ML Flicek P. (2019). "GENCODE reference annotation for the human and mouse genomes." In: *Nucleic Acids Res.* 47.D1, pp. D766–D773.

Love MI Huber W, Anders S. (2014). "Moderated estimation of fold change and dispersion for RNA-seq data with DESeq2." In: *Genome Biol.* 15.12, p. 550.

Subramanian A Tamayo P, Mootha VK Mukherjee S Ebert BL Gillette MA Paulovich A-Pomeroy SL Golub TR-Lander ES Mesirov JP. (2005). "Gene set enrichment analysis: a knowledge-based approach for interpreting genome-wide expression profiles." In: *Proc Natl Acad Sci U S A.* 102.43, pp. 15545–15550.

Zhu A Ibrahim JG, Love MI. (2019). "Heavy-tailed prior distributions for sequence count data: removing the noise and preserving large differences." In: *Bioinformatics.* 35.12, pp. 2084–2092.

Fabregat A Sidiropoulos K, Viteri G Forner O Marin-Garcia P Arnau V D'Eustachio P Stein L Hermjakob H. (2017). "Reactome pathway analysis: a high-performance in-memory approach." In: *BMC Bioinformatics.* 18.1, p. 142.

Liberzon A Birger C, Thorvaldsdóttir H Ghandi M Mesirov JP Tamayo P. (2015). "The Molecular Signatures Database (MSigDB) hallmark gene set collection." In: *Cell Syst.* 1.6, pp. 417–425.

Masica DL, Karchin R. (2011). "Correlation of somatic mutation and expression identifies genes important in human glioblastoma progression and survival." In: *Cancer Res.* 71.13, pp. 4550–4561.

Yang L Huang Y, Zhou L Dai Y Hu G. (2019). "High pretreatment neutrophil-to-lymphocyte ratio as a predictor of poor survival prognosis in head and neck squamous cell carcinoma: Systematic review and meta-analysis." In: *Head Neck..* 41.5, pp. 1525–1535.

Lin Y Xu J, Lan H. (2019). "Tumor-associated macrophages in tumor metastasis: biological roles and clinical therapeutic applications." In: *J Hematol Oncol.* 12.1, p. 76.

Wondergem NE Nauta IH, Muijlwijk T Leemans CR van de Ven R. (2020). "The Immune Microenvironment in Head and Neck Squamous Cell Carcinoma: on Subsets and Subsites." In: *Curr Oncol Rep.* 22.8, p. 81.

Gu-Trantien C Loi S, Garaud S Equeter C Libin M de Wind A Ravoet M Le Buanec H Sibille C Manfouo-Foutsop G Veys I Haibe-Kains B Singhal SK Michiels S Rothé F Salgado R Duvillier H Ignatiadis M Desmedt C Bron D Larsimont D Piccart M Sotiriou C Willard-Gallo K. (2013). "CD4 follicular helper T cell infiltration predicts breast cancer survival." In: *J Clin Invest.* 123.7, pp. 2873–2892.

Lechner A Schlößer HA, Thelen M Wennhold K Rothschild SI Gilles R Quaas A Siefer OG Huebbers CU Cukuroglu E Göke J-Hillmer A Gathof B Meyer MF Klussmann JP Shimabukuro-Vornhagen A Theurich S Beutner D von Bergwelt-Baildon M. (2019). "Tumor-associated B cells and humoral immune response in head and neck squamous cell carcinoma." In: *Oncoimmunology.* 8.3, p. 1535293.

Hu RJ Ma JY, Hu G. (2018). "Lymphocyte-to-monocyte ratio in pancreatic cancer: Prognostic significance and meta-analysis." In: *Clin Chim Acta.* 481.1, pp. 142–146.

Yang YT Jiang JH, Yang HJ Wu ZJ Xiao ZM Xiang BD. (2018). "The lymphocyte-to-monocyte ratio is a superior predictor of overall survival compared to established biomarkers in HCC patients undergoing liver resection." In: *Sci Rep.* 8.1, p. 2535.

Jairath NK Farha MW, Jairath R Harms PW Tsoi LC Tejasvi T. (2020). "Prognostic value of intratumoral lymphocyte-to-monocyte ratio and M0 macrophage enrichment in tumor immune microenvironment of melanoma." In: *Melanoma Manag.* 7.4, MMT51.

Padoan A Plebani M, Basso D. (2019). "Inflammation and Pancreatic Cancer: Focus on Metabolism, Cytokines, and Immunity." In: *Int J Mol Sci.* 20.3, p. 676.

Choo YW Kang M, Kim HY Han J Kang S Lee JR Jeong GJ Kwon SP Song SY Go S Jung M-Hong J Kim BS. (2018). "M1 Macrophage-Derived Nanovesicles Potentiate the Anticancer Efficacy of Immune Checkpoint Inhibitors." In: *ACS Nano.* 12.9, pp. 8977–8993.

Xiao T Xu Z, Zhang H Geng J Qiao Y Liang Y Yu Y Dong Q Suo G. 2019 Jun;52(6):379-384. (2019). "TP53I11 suppresses epithelial-mesenchymal transition and metastasis of breast cancer cells." In: *BMB Rep.* 52.6, pp. 379–384.

Wang Y Liu X, Liu G Wang X Hu R Liang X. (2018). "PIG11 over-expression predicts good prognosis and induces HepG2 cell apoptosis via reactive oxygen species-dependent mitochondrial pathway." In: *Biomed Pharmacother.* 108.1, pp. 435–442.

Liu XM Xiong XF, Song Y Tang RJ Liang XQ Cao EH. (2009). "Possible roles of a tumor suppressor gene PIG11 in hepatocarcinogenesis and As2O3-induced apoptosis in liver cancer cells." In: *J Gastroenterol.* 44.5, pp. 460–460.

Sun Y Zuo Z, Kuang Y. (2020). "An Emerging Target in the Battle against Osteoarthritis: Macrophage Polarization." In: *Int J Mol Sci.* 21.22, p. 8513.

Nie Y Wang Z, Chai G Xiong Y Li B Zhang H Xin R Qian X Tang Z Wu J-Zhao P. (2019). "Dehydrocostus Lactone Suppresses LPS-induced Acute Lung Injury and Macrophage Activation through NF-B Signaling Pathway Mediated by p38 MAPK and Akt." In: *Molecules.* 24.8, p. 1510.

Park JI Song KH, Jung SY Ahn J Hwang SG Kim J Kim EH Song JY. (2019). "Tumor-Treating Fields Induce RAW264.7 Macrophage Activation Via NK-B/MAPK Signaling Pathways." In: *Technol Cancer Res Treat.* 18.1, pp. –.

Islam SU Lee JH, Shehzad A Ahn EM Lee YM Lee YS. (2018). "Decursinol Angelate Inhibits LPS-Induced Macrophage Polarization through Modulation of the NFB and MAPK Signaling Pathways." In: *Molecules.* 23.8, p. 1880.

Affara NI Ruffell B, Medler TR Gunderson AJ Johansson M Bornstein S Bergsland E Steinhoff M Li Y Gong Q-Ma Y-Wiesen JF Wong MH Kulesz-Martin M Irving B-Coussens LM. (2014). "B cells regulate macrophage phenotype and response to chemotherapy in squamous carcinomas." In: *Cancer Cell.* 25.6, pp. 809–821.

Zhang X Li J, Luo S Wang M Huang Q Deng Z de Febbo C Daoui A Liew PX Sukhova GK Metso J Jauhiainen M Shi GP-Guo J. (2020). "IgE Contributes to Atherosclerosis and Obesity by Affecting Macrophage Polarization, Macrophage Protein Network, and Foam Cell Formation." In: *Arterioscler Thromb Vasc Biol.* 40.3, pp. 597–610.

Karagiannis SN Josephs DH, Bax HJ Spicer JF. (2017). "Therapeutic IgE Antibodies: Harnessing a Macrophage-Mediated Immune Surveillance Mechanism against Cancer." In: *Cancer Res.* 77.11, pp. 2779–2783.

Li AJ Li HG, Tang EJ Wu W Chen Y Jiang HH Lin MB Yin L. (2018). "PIK3CA and TP53 mutations predict overall survival of stage II/III colorectal cancer patients." In: *World J Gastroenterol.* 24.5, pp. 613–640.

Chen X Guo Y, Ouyang T Li J Wang T Fan Z Fan T Lin B Xu Y Xie Y. (2019). "Co-mutation of TP53 and PIK3CA in residual disease after neoadjuvant chemotherapy is associated with poor survival in breast cancer." In: *J Cancer Res Clin Oncol.* 145.5, pp. 1235–1242.

Fujimoto Y Morita TY, Ohashi A Haeno H Hakozaki Y Fujii M Kashima Y Kobayashi SS Mukohara T. (2020). "Combination treatment with a PI3K/Akt/mTOR pathway inhibitor overcomes resistance to anti-HER2 therapy in PIK3CA-mutant HER2-positive breast cancer cells." In: *Sci Rep.* 10.1, p. 21762.

Zhang Y Kwok-Shing Ng P, Kucherlapati M Chen F Liu Y Tsang YH de Velasco G Jeong KJ Akbani R Hadjipanayis A Pantazi A Bristow CA-Lee E Mahadeshwar HS-Tang J Zhang J Yang L Seth S-Lee S Ren X Song X Sun H Seidman J Luquette LJ Xi R Chin L Protopopov A Westbrook TF Shelley CS Choueiri TK Ittmann M Van Waes C Weinstein JN Liang H Henske EP Godwin AK Park PJ Kucherlapati R Scott KL Mills GB-Kwiatkowski DJ Creighton CJ. (2017). "A Pan-Cancer Proteogenomic Atlas of PI3K/AKT/mTOR Pathway Alterations." In: *Cancer Cell.* 31.6, pp. 820–832.

O'Donnell JS Massi D, Teng MWL Mandala M. (2018). "PI3K-AKT-mTOR inhibition in cancer immunotherapy, redux." In: *Semin Cancer Biol.* 48.1, pp. 91–103.

Okkenhaug K Graupera M, Vanhaesebroeck B. (2016). "Targeting PI3K in Cancer: Impact on Tumor Cells, Their Protective Stroma, Angiogenesis, and Immunotherapy." In: *Cancer Discov.* 6.10, pp. 1090–1105.

Sonnenblick A Venet D, Brohée S Pondé N Sotiriou C. (2019). "pAKT pathway activation is associated with PIK3CA mutations and good prognosis in luminal breast cancer in contrast to p-mTOR pathway activation." In: *NPJ Breast Cancer.* 5.1, p. 7.

Vergadi E Ieronymaki E, Lyroni K Vaporidi K Tsatsanis C. (2017). "Akt Signaling Pathway in Macrophage Activation and M1/M2 Polarization." In: *J Immunol.* 198.3, pp. 1006–1014.

Xie S Chen M, Yan B He X Chen X Li D. (2014). "Identification of a role for the PI3K/AKT/mTOR signaling pathway in innate immune cells." In: *PLoS One.* 9.4, e94496.

Kumar AT Knops A, Swendseid B Martinez-Outschoom U Harshyne L Philp N Rodeck U Luginbuhl A Cognetti D Johnson J Curry J. 2019 Jul 23;9:656. (2019). "Prognostic Significance of Tumor-Associated Macrophage Content in Head and Neck Squamous Cell Carcinoma: A Meta-Analysis." In: *Front Oncol.* 9.1, p. 656.

S., Crotty (2014). "T follicular helper cell differentiation, function, and roles in disease." In: *Immunity.* 41.4, pp. 529–542.

GS., Wu (2004). "The functional interactions between the p53 and MAPK signaling pathways." In: *Cancer Biol Ther.* 3.2, pp. 156–161.

Gulati AP Yang YM, Harter D Mukhopadhyay A Aggarwal BB Benzil DL Whysner J Albino AP Murali R Jhanwar-Uniyal M. (2006). "Mutant human tumor suppressor p53 modulates the activation of mitogen-activated protein kinase and nuclear factor-kappaB, but not c-Jun N-terminal kinase and activated protein-1." In: *Mol Carcinog.* 45.1, pp. 26–37.

Brown L, Benchimol S. 2006 Feb 17;281(7):3832-40. (2006). "The involvement of MAPK signaling pathways in determining the cellular response to p53 activation: cell cycle arrest or apoptosis." In: *J Biol Chem.* 281.7, pp. 3832–3840.

Bueter M Gasser M, Schramm N Lebedeva T Tocco G Gerstlauer C Grimm M Nichiporuk E Thalheimer A Thiede A Meyer D Benichou G Waaga-Gasser AM. (2006). "T-cell response to p53 tumor-associated antigen in patients with colorectal carcinoma." In: *Int J Oncol.* 28.2, pp. 431–438.

Huang YH Chen MH, Guo QL Chen ZX Chen QD Wang XZ. (2020). "Interleukin-10 induces senescence of activated hepatic stellate cells via STAT3-p53 pathway to attenuate liver fibrosis." In: *Cell Signal.* 66.1, p. 109445.

Blagih J Zani F, Chakravarty P Hennequart M Pilley S Hobor S Hock AK Walton JB Morton JP Gronroos E Mason S Yang M McNeish I Swanton C Blyth K Vousden KH. (2020). "Cancer-Specific Loss of p53 Leads to a Modulation of Myeloid and T Cell Responses." In: *Cell Rep.* 30.2, pp. 481–496.

Liu G Park YJ, Tsuruta Y Lorne E Abraham E. (2009). "p53 Attenuates lipopolysaccharide-induced NF-kappaB activation and acute lung injury." In: *J Immunol.* 182.8, pp. 5063–5071.

Murphy SH Suzuki K, Downes M Welch GL De Jesus P Miraglia LJ Orth AP Chanda SK Evans RM Verma IM. (2011). "Tumor suppressor protein (p)53, is a regulator of NF-kappaB repression by the glucocorticoid receptor." In: *Proc Natl Acad Sci U S A.* 108.41, pp. 17117–17122.

Vaughan CA Singh S, Windle B Sankala HM Graves PR Andrew Yeudall W Deb SP Deb S. (2012). "p53 mutants induce transcription of NF-B2 in H1299 cells through CBP and STAT binding on the NF-B2 promoter and gain of function activity." In: *Arch Biochem Biophys.* 518.1, pp. 79–88.

Schulze-Osthoff K Ferrari D, Riehemann K Wesselborg S. (1997). "Regulation of NF-kappa B activation by MAP kinase cascades." In: *Immunobiology.* 198.1-3, pp. 35–49.

Pascarella A Bracaglia C, Caiello I Arduini A Moneta GM Rossi MN Matteo V Pardeo M De Benedetti F Prencipe G. (2021). "Monocytes From Patients With Macrophage Activation Syndrome and Secondary Hemophagocytic Lymphohistiocytosis Are Hyperresponsive to Interferon Gamma." In: *Front Immunol.* 17.1, p. 663329.

Huangfu N Zheng W, Xu Z Wang S Wang Y Cheng J Li Z Cheng K Zhang S Chen X Zhu J. (2020). "RBM4 regulates M1 macrophages polarization through targeting STAT1-mediated glycolysis." In: *Int Immunopharmacol.* 83.1, p. 106432.

Sikora J Dworacki G, Giersz R Zeromski J. (2004). "The role of monocytes/macrophages in TCR-zeta chain downregulation and apoptosis of T lymphocytes in malignant pleural effusions." In: *J Biol Regul Homeost Agents.* 18.1, pp. 26–32.

Ezernitchi AV Vaknin I, Cohen-Daniel L Levy O Manaster E Halabi A Pikarsky E Shapira L Baniyash M. (2006). "TCR zeta down-regulation under chronic

inflammation is mediated by myeloid suppressor cells differentially distributed between various lymphatic organs." In: *J Immunol.* 177.7, pp. 4763–4772.

Kent L.N., Leone G. (2019). "The broken cycle: E2F dysfunction in cancer." In: *Nat Rev Cancer.* 1.1, pp. 326–338.

Scott LE Weinberg SH, Lemmon CA. (2019). "Mechanochemical Signaling of the Extracellular Matrix in Epithelial-Mesenchymal Transition." In: *Front Cell Dev Biol.* 7.1, p. 135.